Research Article
Vol. 26, No. 11 | 28 May 2018 | OPTICS EXPRESS 14267
Optics EXPRESS

Two-step algorithm for removing the rotationally asymmetric systemic errors on grating lateral shearing interferometer

LU ZHANG,[1,2] KEQI QI,[1] AND YANG XIANG[1,*]
[1]State Key Laboratory of Applied Optics, Changchun Institute of Optics, Fine Mechanics and Physics, Chinese Academy of Sciences, Changchun, 130033, Jilin, China
[2]University of Chinese Academy of Sciences, Beijing, 100049, China
*y.xiang@sklao.ac.cn

Abstract: The grating lateral shearing interferometer may achieve ultra-high accuracy absolute testing after eliminating the systemic errors from the interferometer itself and the orthogonality problem between two shearing directions. Aiming at the interferometer, we proposed a two-step algorithm for removing the rotationally asymmetric systemic errors from our shearing setup. This rotation method provides a new approach for acquiring the wavefront aberration by choosing the rotation angles with the minimum decentration and to satisfy the immune of systemic errors at the same time. Simulation and experiment verified that it is more propitious to eliminate the systemic errors when it is applied to our shearing setup.

OCIS codes: (120.3180) Interferometry; (120.3940) Metrology; (120.4800) Optical standards and testing.

References and links

1. D. Malacara, “Phase shifting interferometry,” in *Optical Shop Testing*, 2nd ed. (Wiley, 1992), Chap.14.
2. A. E. Jensen, “Absolute calibration method for Twyman–Green wavefront testing interferometers,” J. Opt. Soc. Am. **63**, 1313A (1973).
3. K. Creath and J. C. Wyant, “Testing spherical surfaces: a fast, quasi-absolute technique,” Appl. Opt. **31**(22), 4350–4354 (1992).
4. R. E. Parks, “Removal of test optics errors,” Proc. SPIE **153**, 56–63 (1978).
5. B. S. Fritz, “Absolute calibration of an optical flat,” Opt. Eng. **23**(4), 379–383 (1984).
6. C. J. Evans and R. N. Kestner, “Test optics error removal,” Appl. Opt. **35**(7), 1015–1021 (1996).
7. H.-G. Rhee, Y.-W. Lee, and S. W. Kim, “Azimuthal position error correction algorithm for absolute test of large optical surfaces,” Opt. Express **14**(20), 9169–9177 (2006).
8. E. E. Bloemhof, “Absolute surface metrology by differencing spatially shifted maps from a phase-shifting interferometer,” Opt. Lett. **35**(14), 2346–2348 (2010).
9. W. Song, F. Wu, and X. Hou, “Method to test rotationally asymmetric surface deviation with high accuracy,” Appl. Opt. **51**(22), 5567–5572 (2012).
10. D. Su, E. Miao, Y. Sui, and H. Yang, “Absolute surface figure testing by shift-rotation method using Zernike polynomials,” Opt. Lett. **37**(15), 3198–3200 (2012).
11. Y. Zhang, D. Su, L. Li, Y. Sui, and H. Yang, “Error-immune Algorithm for Absolute Testing of Rotationally Asymmetric Surface Deviation,” J. Opt. Soc. Korea **18**(4), 335–340 (2014).
12. W. Wang, M. Zhang, S. Yan, Z. Fan, and J. Tan, “Absolute spherical surface metrology by differencing rotation maps,” Appl. Opt. **54**(20), 6186–6189 (2015).
13. Z. G. Han, L. Yin, L. Chen, and R. H. Zhu, “Absolute flatness testing of skip-flat interferometry by matrix analysis in polar coordinates,” Appl. Opt. **55**(9), 2387–2392 (2016).
14. Z. Yang, J. Du, C. Tian, J. Dou, Q. Yuan, and Z. Gao, “Generalized shift-rotation absolute measurement method for high-numerical-aperture spherical surfaces with global optimized wavefront reconstruction algorithm,” Opt. Express **25**(21), 26133–26147 (2017).
15. J. M. Bueno, E. Acosta, C. Schwarz, and P. Artal, “Wavefront measurements of phase plates combining a point-diffraction interferometer and a Hartmann-Shack sensor,” Appl. Opt. **49**(3), 450–456 (2010).
16. C. Ouchi, S. Katoa, and M. Hasegawa, “EUV wavefront metrology at EUVA,” Proc. SPIE **6152**, 61522 (2006).
17. J. C. Wyant, “Double frequency Grating Lateral Shear Interferometer,” Appl. Opt. **12**(9), 2057–2060 (1973).
18. H. Schreiber and J. Schwider, “Lateral shearing interferometer based on two Ronchi phase gratings in series,” Appl. Opt. **36**(22), 5321–5324 (1997).
19. S. Kato, C. Ouchi, M. Hasegawa, A. Suzuki, T. Hasegawa, K. Sugisaki, M. Okada, Z. Yucong, K. Murakami, J. Saito, M. Niibe, and M. Takeda, “Comparison of EUV interferometry methods in EUVA project,” Proc. SPIE **5751**, 110–117 (2005).

#327159
https://doi.org/10.1364/OE.26.014267
Journal © 2018
Received 2 Apr 2018; revised 26 Apr 2018; accepted 27 Apr 2018; published 21 May 2018

Optics EXPRESS

20. H. G. Rhee, Y. S. Ghim, J. Lee, H. S. Yang, and Y. W. Lee, "Correction of rotational inaccuracy in lateral shearing interferometry for freeform measurement," Opt. Express **21**(21), 24799–24808 (2013).

1. Introduction

In surface measurements, absolute testing technique [1] is a common method for measuring the surface deviation, which can get the absolute surface information without the effect due to the reference surface. Concerning absolute testing, Jensen had proposed a two-sphere method [2] for optical spherical surface absolute testing. And then many novel approaches [3–14] about absolute testing have been presented, such as the single-rotation algorithm [4] and the rotation-averaging algorithm [5]. In addition, absolute testing can also be used to measure the wavefront aberration of lithographic lens. Lithographic lens, the core component of lithography machine, need to acquire its wavefront aberration by ultra-high accuracy measurement equipment. The major methods for testing the lithographic lens are Shark-Hartmann Interferometry [15], Point Diffraction Interferometry [16], and Grating Shearing Interferometry [17–19]. For the lithographic lens in 193nm work wavelength, we usually utilize grating lateral shearing interferometry to measure the wavefront aberration of the lens, owing to the rigorous working condition and the costly expenses. For convenience, we usually use the ordinary projection lens in our experiment. However, the grating lateral shearing interferometer [17–19] may achieve ultra-high accuracy absolute testing after removing the systemic errors from our shearing setup and the orthogonality problem between two shearing directions. Then the latter problem had been solved by a new algorithm [20] that is able to compensate the rotational inaccuracy, so we aim of the former in this paper. According to the principle of absolute calibration, some algorithms doesn't work on the grating lateral shearing interferometer, which is shown in Fig. 1, such as the cat's eye method [1–3] and the shift method [10], and we can only use the rotation algorithms to ensure the systemic errors from the interferometer.

At these series of rotation measurement methods, for the single-rotation algorithm [4], the accuracy is unstable because the rotation angle with minimum error is determined by the difference of variational errors and is very hard to predict; and for the rotation-averaging method [5], it has a quite high accuracy because it can average random errors, but it need more rotation measurements in order to get necessary information. By the contrastive study, error-immune algorithm [11] can characterize the wavefront aberration of the lens under test better. Based on least-square fitting of Zernike polynomials, it makes combinations of multiple evaluations of four angular components of a surface into a final calibration data. But for the sketch of shearing setup shown in Fig. 1, whose diameters of the rotating platform are 0.65 m and over, the unsuitable rotation angles may bring about the large decentration, and then it may change the whole optical path because of grating shearing.

Optics EXPRESS

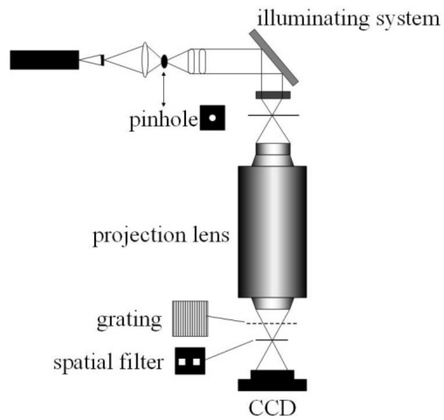

Fig. 1. The sketch of grating lateral shearing interferometer.

In this paper, we proposed a two-step method based on error-immune algorithm [11]. The theoretical formulas are derived in Section 2, and the simulation and the experimental results about new algorithm are presented in Section 3. Finally, some conclusions are given in Section 4.

2. Theoretical analysis

The wavefront aberration of the lens under test acquired in original position can be expressed as:

$$W(\rho,\theta)=W_s(\rho,\theta)+T(\rho,\theta)+V(\rho,\theta) \tag{1}$$

where $W_s(\rho,\theta)$ is the constant systemic errors from interferometer; $T(\rho,\theta)$ is the wavefront aberration from the lens under test; $V(\rho,\theta)$ is the variable systemic errors including environmental disturbance, azimuthal errors, decentration errors, and so on.

Then the lens under test is rotated about the optical axis by an angle φ, and the wavefront aberration can be expressed as

$$W(\rho,\theta+\varphi)=W_s(\rho,\theta)+T(\rho,\theta+\varphi)+V'(\rho,\theta) \tag{2}$$

Subtracting Eq. (1) from Eq. (2), we get

$$\Delta W(\rho,\theta)=T(\rho,\theta+\varphi)-T(\rho,\theta)+\Delta V(\rho,\theta) \tag{3}$$

By Zernike polynomials, the result in Eq. (3) can be written as:

$$\begin{aligned}\Delta W(\rho,\theta)=&\sum_{m,n}R_n^m(\rho)\{a_n^m\cos[m(\theta+\varphi)]-a_n^m\cos(m\theta)\\&+a_n^m\sin[m(\theta+\varphi)]-a_n^m\sin(m\theta)\}+\Delta V(\rho,\theta)\\=&\sum_{m,n}R_n^m(\rho)[\alpha_n^{m,\varphi}\cos(m\theta)+\alpha_n^{-m,\varphi}\sin(m\theta)]+\Delta V(\rho,\theta)\end{aligned} \tag{4}$$

where, $\alpha_n^{m,\phi}=a_n^m[\cos(m\phi)-1]+a_n^{-m}\sin(m\phi)$; $\alpha_n^{-m,\phi}=a_n^{-m}[\cos(m\phi)-1]-a_n^m\sin(m\phi)$.

According to the error-immune algorithm [11], the influence of $\Delta V(\rho,\theta)$ can be reduced by optimal angles: When $\cos(m\phi)=-1$, the error sensitivity is the least and those rotation angles matching $\cos(m\phi)=-1$ are called optimal angles. Optimal angles are completely decided by angular order m. When we characterize the variable systemic errors by a 36-term Zernike polynomials, it need to respectively rotate the lens by 0°, 90°, 135°, and 180°. And

Optics EXPRESS

we can get: 2θ Zernike coefficients by 90°; 4θ Zernike coefficients by 135°; odds θ Zernike coefficients by 180°.

However,it is on the grating lateral shearing interferometer that the variable systemic errors cannot be simply reduced by optimal angles because the tiny decentration may change the whole optical path. The total wavefront aberration in X direction we measured from original position can expressed as

$$W(x,y)=W_{-1}(x+s/2,y)-W_{+1}(x-s/2,y) \tag{5}$$

where $W_{-1}(x,y)$ and $W_{+1}(x,y)$ respectively are the wavefront aberrations of ± 1 order diffraction light.

Then the lens is rotated by an angle φ, the center of lens and the position of interferograms will be shifted for the influence of decentration, and the phase of the corresponding position will be also changed in original light path because of grating shearing. The total wavefront aberration will become to

$$W'(x,y)=W_{-1}'(x+s/2+\Delta x,y+\Delta y)-W_{+1}'(x-s/2+\Delta x,y+\Delta y) \tag{6}$$

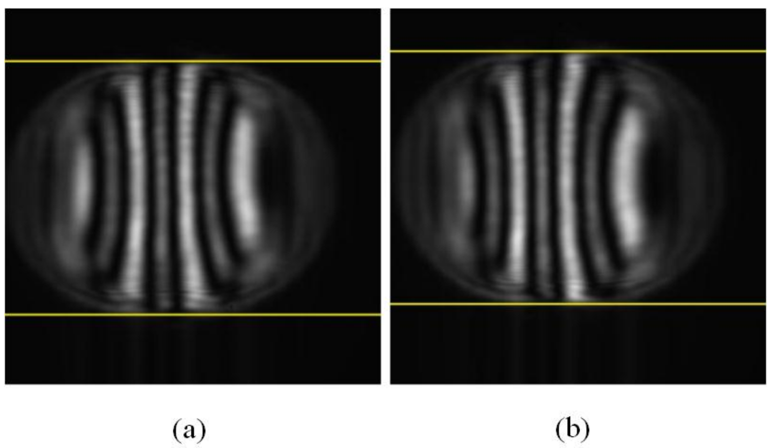

Fig. 2. The interferograms in X orientation: (a) at the 0° position; (b) at the 180° position.

Similarly, the position of interferograms in Y orientation will also be shifted by the rotation of the lens. The position of interferograms by rotating 180° is obviously different from the original position, as shown in Fig. 2. Then the size of wavefront aberration from the lens under test will be changed by the excursion, and the systemic errors from shearing setup may also be altered by the phase change. The calculation process will be complex to the variable systemic errors as shown in Eqs. (5) and (6). We need to pick out the appropriate angles to consider the decentration and to satisfy the immune of systemic errors at the same time. The theoretical analyses about new algorithm are shown as following:

We rotate the lens under test about the optical axis by 8 equally spaced angles then acquire the wavefront aberrations at these positions.

The sum of the 8 positions wavefront aberrations can be written as

$$\sum_{j=0}^{N-1} W_j(\rho,\theta)=\sum_{j=0}^{N-1} T_j(\rho,\theta)+8\cdot W_s(\rho,\theta)+\sum_{j=0}^{N-1} V_j(\rho,\theta) \tag{7}$$

where the sum of $V_j(x,y)$ can be neglected by the mean of 8 times measurement, because the variable systemic errors may be averaged by a periodic rotation, and the N is the times of rotation.

Then Eq. (7) will become to

$$\begin{aligned}\sum_{j=0}^{N-1} W_j(\rho,\theta) &= \sum_{j=0}^{N-1} T_j(\rho,\theta) + 8\cdot W_s(\rho,\theta)\\ &= \sum_{j=0}^{N-1} T_j^{1,3,5}(\rho,\theta) + \sum_{j=0}^{N-1} T_j^{2}(\rho,\theta) + \sum_{j=0}^{N-1} T_j^{4}(\rho,\theta) + 8\cdot W_s(\rho,\theta)\\ &= 0+0+0+8\cdot W_s(\rho,\theta)\end{aligned} \tag{8}$$

where the superscript numbers in Eq. (8) represent the angular order m from the 36-term Zernike polynomials.

We can get the wavefront aberration contains the variable systemic errors

$$x_j(\rho,\theta) = T_j(\rho,\theta) + V_j(\rho,\theta) = W_j(\rho,\theta) - \frac{1}{8}\sum_{j=0}^{N-1} W_j(\rho,\theta) \tag{9}$$

Then the function used to confirm the original position (0°) with the least decentration is given by

$$\phi_0 = \arg\max_{\phi} \frac{\sum_\rho \sum_\theta [x(\rho,\theta+\phi) - x(\rho,\theta+\phi+180°)]^2}{\sum_\rho \sum_\theta [x(\rho,\theta+\phi) - x(\rho,\theta+\phi+45°)]^2 + \sum_\rho \sum_\theta [x(\rho,\theta+\phi) - x(\rho,\theta+\phi-45°)]^2} \tag{10}$$

where $x(\rho,\theta)$ represents the wavefront aberration contains the variable systemic errors at a random angular position we measured for the first time; ϕ is the rotation angle relative to this random angular position. The original position is determined with the rotation angle ϕ_0 satisfying Eq. (10).

The next step is to choose the angles with the minimum decentration near from the original position. For the error-immune algorithm [11], the 180° from the optimal angles, which satisfy $\cos(m\phi) = -1$, will have the maximum decentration in our algorithm, so we can replace 180° with 90° or 270° because these angles must be used to get other angular order m = 2 and have still less decentration. When φ = 90° or φ = 270°, for the odd angular order, Eq. (4) will become to

$$\begin{aligned}\Delta W_{odd}(\rho,\theta) &= W_{odd}{}'(\rho,\theta) - W_{odd}(\rho,\theta)\\ &= \sum_{m,n} R_n^m(\rho)[\alpha_n^{m,\pm\pi/2}{}_{odd}\cos(m\theta) + \alpha_n^{-m,\pm\pi/2}{}_{odd}\sin(m\theta)] + \Delta V(\rho,\theta)\end{aligned} \tag{11}$$

where, $\alpha_n^{m,\pm\pi/2}{}_{odd} = -a_n^m + a_n^{-m}\sin(\pm m\pi/2)$; $\alpha_n^{-m,\pm\pi/2}{}_{odd} = -a_n^{-m} - a_n^m\sin(\pm m\pi/2)$.

Therefore, for the first 36 terms in the Zernike polynomial, we may get: 2θ Zernike coefficients by 90° or 270°; 4θ Zernike coefficients by 45° or 315°; and odds θ Zernike coefficients by 90° or 270°. Then we verify the choices of angles in the Section 3.

3. Simulation and experiment

The new proposed method has been tested to verify its advantages and accuracy through computer simulation. At the original position, the real wavefront aberrations we simulate is shown in Fig. 3(a), and the wavefront aberrations contains the systemic errors is shown in Fig. 3(b). Then we appropriately mix in variable systemic errors in different rotational angles. The results acquired by error-immune algorithm [11] and the new algorithm, which are expressed by the 36-term Zernike polynomials, are respectively shown in Figs. 3(c) and 3(d).

Optics EXPRESS

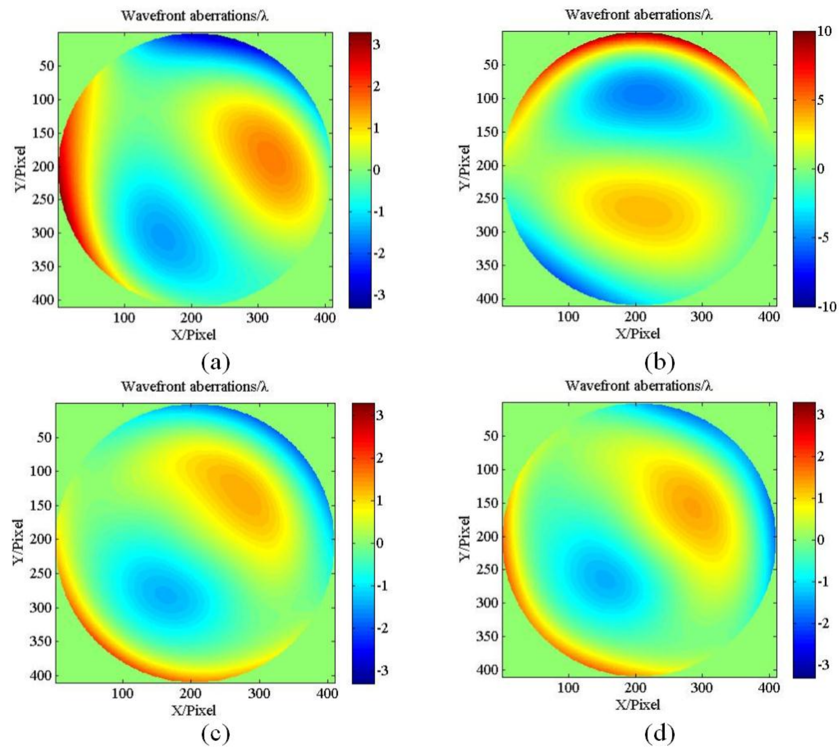

Fig. 3. Immunization capabilities of variable systemic errors about two algorithms: (a) The real wavefront aberrations generated for simulation with random Zernike coefficients for m = 1-5 (PV: 6.2757λ; RMS: 0.9758λ); (b) The wavefront aberrations contains the systemic errors (PV: 16.182λ; RMS: 2.6038λ); (c) The wavefront aberrations acquired by error-immune algorithm with the angles being 0°, 90°, 135°, and 180° (PV: 4.0146λ; RMS: 0.73895λ); (d) The wavefront aberrations acquired by new algorithm with the angles being 0°, 90°, and 315° (PV: 3.784λ; RMS: 0.73364λ).

The residuals between the real wavefront aberrations and the wavefront aberrations acquired by these two algorithms are shown in Fig. 4. According to the PV and RMS value of residuals, we can obtain that the wavefront aberrations by new algorithm is more close to the real wavefront aberrations. It is thus clear that the accuracy of new algorithm may higher while the variable systemic errors are inevitable.

In the experiment, we verify this new algorithm on grating lateral shearing interferometer as shown in Fig. 1, the wavelength of optical source is 632.8 nm. Then through the grating, we realize the shearing interferometry by the ± 1 order diffraction light which are acquired by spatial filter. In order to ensure the original position with the least decentration, we respectively measure the shearing interferograms of two orthogonal directions at 8 equally spaced angular positions rotating about the optical axis. The wavefront aberrations at eight angular positions are acquired by wavefront reconstruction and the algorithm [20] that is able to compensate the rotational inaccuracy. And then the original position is ascertained by Eq. (10). The PV and RMS values of wavefront aberrations at eight angular positions are shown in Fig. 5 before systemic errors elimination and after systemic errors elimination.

Optics EXPRESS

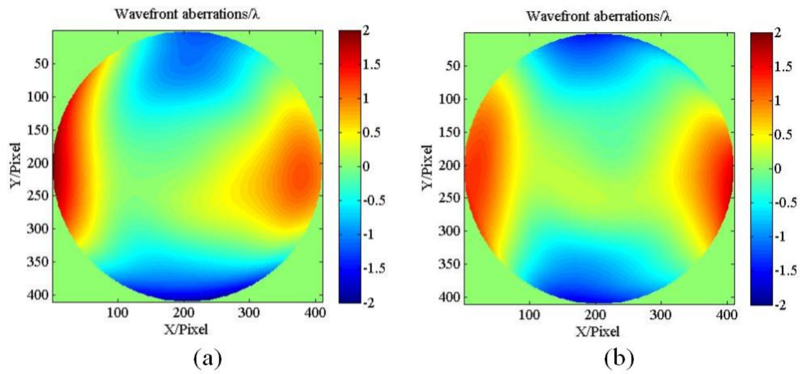

Fig. 4. Comparison of two algorithms: The residuals between the original wavefront aberrations and (a) the wavefront aberrations acquired by error-immune algorithm (PV: 3.9117λ; RMS: 0.68021λ); (b) the wavefront aberrations acquired by new algorithm (PV: 3.3947λ; RMS: 0.64313λ).

We can see that the PVs near 180° position are different from other angular positions in the Fig. 5, and it means the volume of excursion will impact the experimental result at some angular positions. For testifying the influence about the excursion and the accuracy, we try to make a comparison of several different single-rotation algorithms [4].

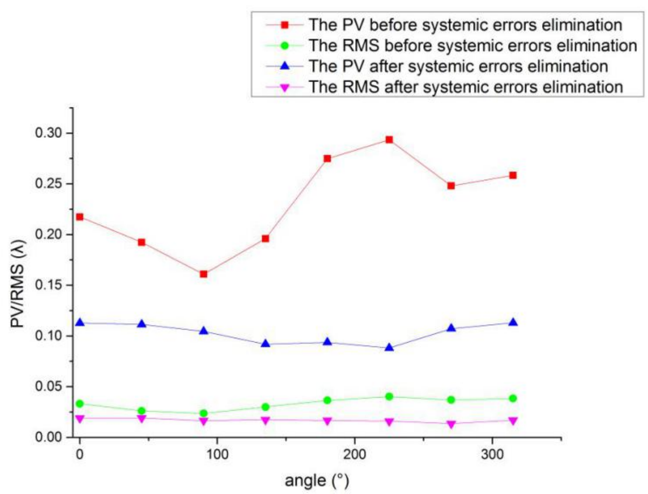

Fig. 5. The PV and RMS values of the wavefront aberrations at eight angular positions before systemic errors eliminated and after systemic errors eliminated by average-rotation algorithm.

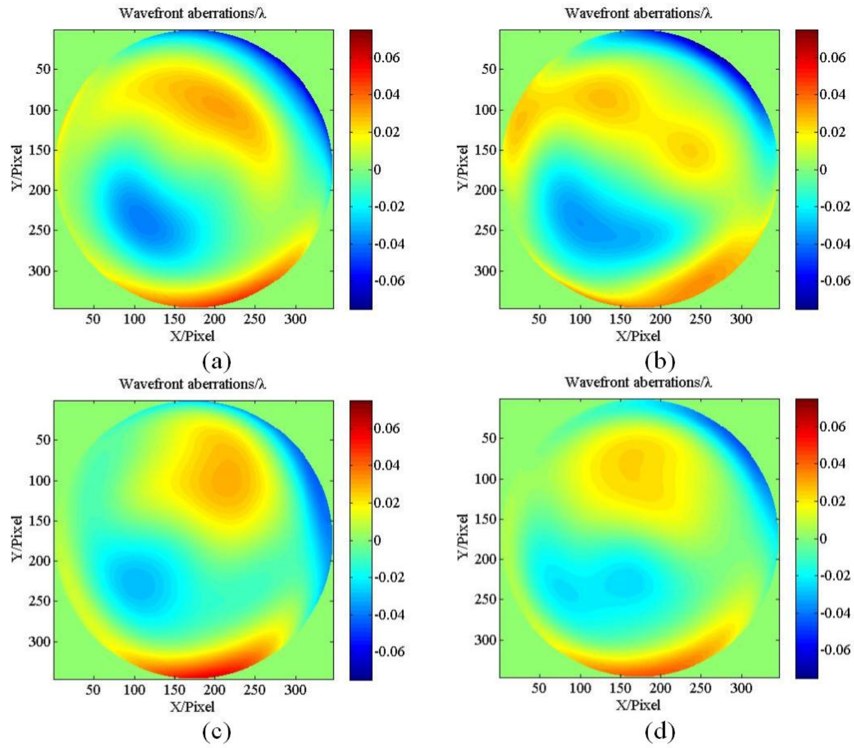

Fig. 6. The wavefront aberrations acquired by different single-rotation algorithms: (a) 45° (b) 135° (c) 225° (d) 315°.

From Figs. 6, it can be clearly seen that there are large difference to the results that are calculated by different single-rotation algorithms, and it also verified the instability about single-rotation algorithm on our shearing setup. To contrast the accuracy of these, we calculate the residuals of wavefront aberrations at two angular positions in different single-rotation algorithms, which are shown in Table 1. These data show that the accuracy of the single-rotation methods varying with the rotation angles, and we can see the change of the decentration and the RMS values by different single-rotation algorithms, which is shown in Fig. 7.

Table 1. The PV and RMS residuals of wavefront aberrations at two angular positions in different single-rotation algorithms.

	Decentration(pixel)	PV(λ)	RMS(λ)
45°	13.45	0.012809	0.0017594
135°	29.00	0.012854	0.0038338
225°	30.27	0.017451	0.0029670
315°	12.08	0.006013	0.0011555

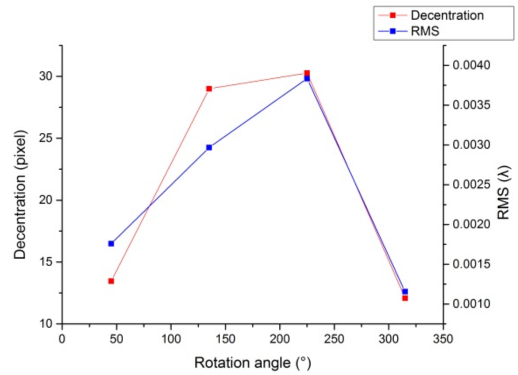

Fig. 7. The decentration and the RMS value of residuals of two wavefronts errors acquired by different single-rotation algorithms.

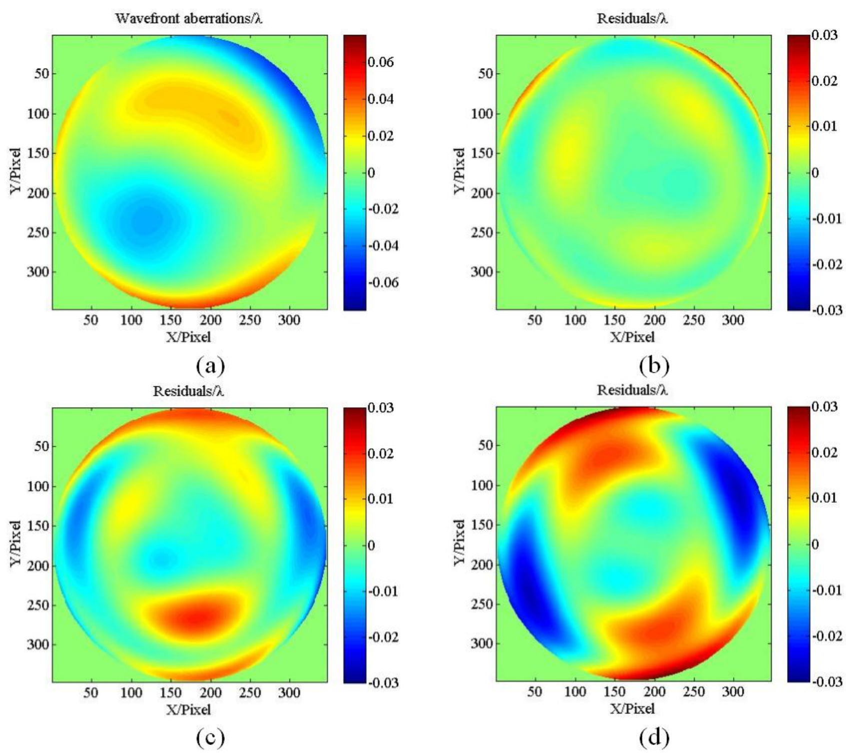

Fig. 8. The result acquired by error-immune algorithm: (a) The wavefront aberrations of the lens on 0° position. The residuals between 0° position and: (b) 90° position (PV: 0.029128λ; RMS: 0.0031796λ); (c) 135° position (PV: 0.042076λ; RMS: 0.0077323λ); (d) 180° position (PV: 0.056729λ; RMS: 0.01229λ).

As we all know, the error-immune algorithm has quite stability and accuracy comparing with the single-rotation algorithm. But this method needs a limiting condition for rotation angles, which may cause a large decentration of the shearing interferograms. For the error-immune algorithm, the wavefront aberrations of the lens at 0° position are shown in Fig. 8(a), and then the residuals of wavefront aberrations between 0° position and other three positions are respectively shown in Figs. 8(b)-8(d). Obviously, the PV and RMS of the residuals largely varied with the rotation angles, and it means the imperfect accuracy of error-immune algorithm on the grating lateral shearing interferometer.

Optics EXPRESS

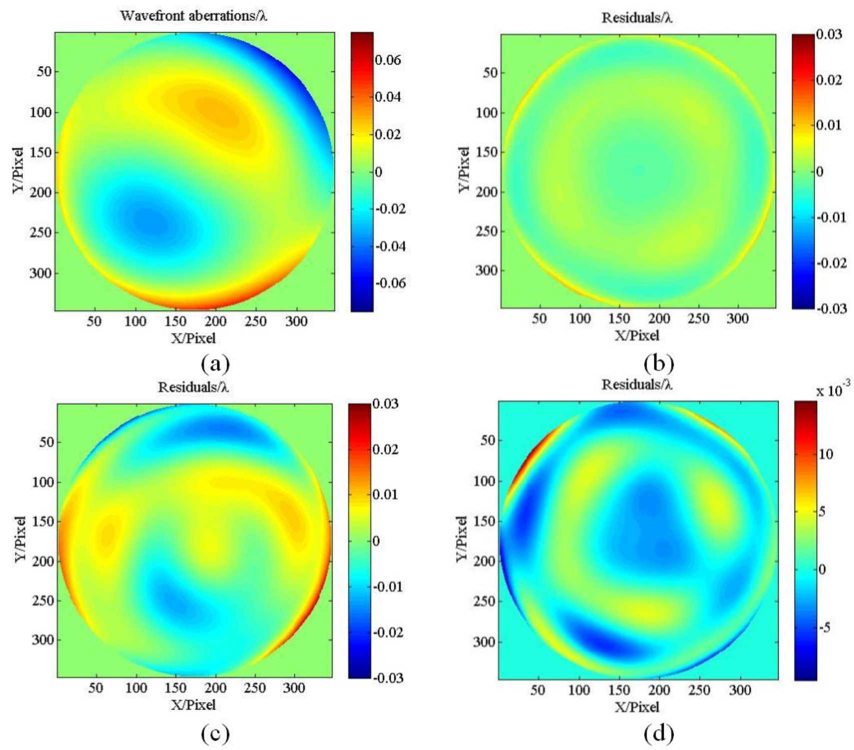

Fig. 9. The result acquired by new algorithm: (a) The systemic errors of the lens on original position. The residuals between 0° position and: (b) 315° position (PV: 0.016595λ; RMS: 0.0023007λ); (c) 90° position (PV: 0.046724λ; RMS: 0.0065709λ); (d) the difference of wavefront aberrations at 0° position between new algorithm and error-immune algorithm (PV: 0.024148λ; RMS: 0.0025226λ).

According to the decentration of the shearing interferograms, new algorithm chooses the three angles, which are 0°, 90° and 315°, to calculate the wavefront aberrations of the lens under test. The wavefront aberrations at 0° position are shown in Fig. 9(a), and then the residuals between 0° position and other positions are shown in Figs. 9(b) and 9(c). The difference of wavefront aberrations between error-immune algorithm and new algorithm at 0° position are shown in Fig. 9(d).

Comparing with the results from error-immune algorithm and new algorithm, the residuals PV and RMS of the latter are entirely less than the former, and then we find new algorithm has a higher accuracy on grating lateral shearing interferometer. Meanwhile, it illustrates that appropriate rotation angles may decrease the variable systemic errors caused by large decentration in optical system. The residual figure in Fig. 9(d) reflects the difference of wavefront aberrations between new algorithm and error-immune algorithm, it also prove verity of the result we simulated at the fore. Then Fig. 10 shows the difference of the 36-term Zernike polynomials acquired by these two methods. From which, we can see that the absolute result of the new method is very close to that of the error-immune algorithm which meets well with above theoretical analysis.

Optics EXPRESS

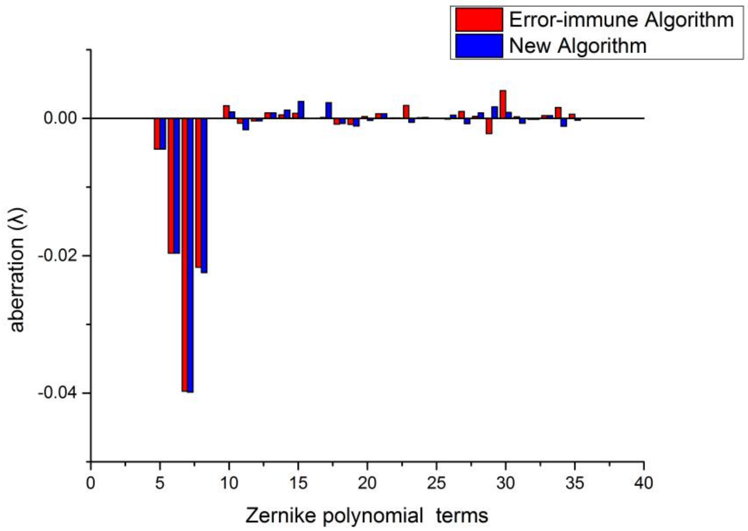

Fig. 10. Comparison of the first 36 terms in the Zernike polynomial between error-immune algorithm and new algorithm.

4. Conclusions

The algorithm we proposed can remove the rotationally asymmetric systemic errors on our shearing setup by these two steps: we confirm the original position (0°) with the least decentration; and then we choose the angles with the minimum decentration and to satisfy the immune of systemic errors at the same time. This method based on error-immune algorithm, and it can decrease the influence of variable systemic errors by choosing the best rotation angles. Comparing with traditional rotation algorithms, new algorithm has less times rotation and more suitable angles to process the large decentration of the lens. Therefore, it can be more propitious to remove the systemic errors on grating lateral shearing interferometer.

Funding

Ministry of Science and Technology of the People's Republic of China (MOST); The 02 National Science and Technology Major Project (2009ZX02202005).